



ELSEVIER

doi:10.1016/j.gca.2004.10.009

High-resolution historical records from Pettaquamscutt River basin sediments: 1. ^{210}Pb and varve chronologies validate record of ^{137}Cs released by the Chernobyl accident

ANA LÚCIA LIMA,^{1,*} J. BRADFORD HUBENY,² CHRISTOPHER M. REDDY,¹ JOHN W. KING,² KONRAD A. HUGHEN,¹
AND TIMOTHY I. EGLINTON¹

¹Department of Marine Chemistry and Geochemistry, Woods Hole Oceanographic Institution, Woods Hole, MA 02543, USA

²Graduate School of Oceanography, University of Rhode Island, Narragansett, RI 02882, USA

(Received January 27, 2004; accepted in revised form October 14, 2004)

Abstract—Cesium-137 derived from the explosion of the Chernobyl reactor in 1986 was preserved in anoxic sediments from a coastal environment in southern Rhode Island. Although the radioactive plume was detected in surface air samples at several locations in the United States, this is the first known record of a Chernobyl ^{137}Cs peak in sediments from North America. The inventory of Chernobyl ^{137}Cs that was preserved in the Pettaquamscutt River is small compared to European counterparts and should only be detectable for the next 15–20 yr. However, the presence of two ^{137}Cs peaks (1963 and 1987) identifies a well-dated segment of the sediment column that could be exploited in understanding the decomposition and preservation of terrestrial and aquatic organic matter. Different methods for calculating the ^{210}Pb chronology were also evaluated in this study and checked against independent varve counting. The end result is a detailed chronology of a site well suited for reconstruction of historical records of environmental change. Copyright © 2005 Elsevier Ltd

1. INTRODUCTION

On April 26, 1986, a flaw in design and a series of operator actions caused the Chernobyl-4 reactor to explode during a test to determine how long the turbines would spin after a loss of electrical power supply. The initial release of fission products to the atmosphere was followed by a second explosion, which allowed air to flow into the core and caused the graphite moderator to burst into flames (Hohenemser et al., 1986; Mould, 2000). The nine-day fire that followed was responsible for the main release of radioactivity into the environment. Roughly all of the xenon gas, 20% of the cesium and iodine, and ~5% of the remaining radioactive material in the reactor was set free by the accident, accounting for a release of more than 8×10^{18} Bq (1 becquerel = 1 disintegration per second) of fission products into the atmosphere (Mould, 2000) (<http://www.world.nuclear.org>). While most of the released material was deposited close to the site of the accident in northern Ukraine, southern Belarus and Russia's Bryansk region (Stone, 2001), strong winds carried a plume towards Finland and Sweden (ApSimon and Wilson, 1986; Mould, 2000). By May 2, the plume had reached the UK and Japan, and by May 6, Canada and the United States (Ayoama et al., 1986; Smith and Clark, 1986; Mould, 2000). Even though ^{137}Cs was detected in the atmosphere in several regions of the United States following the accident (Larsen et al., 1986; Feely et al., 1988; Holloway and Liu, 1988), no record of a clear Chernobyl ^{137}Cs peak is observed in sediments from Florida (Robbins et al., 2000), Massachusetts (Spliethoff and Hemond, 1996), California (Fuller et al., 1999) or other locations in the country (Van Metre et al., 1997). However, a discernible Chernobyl ^{137}Cs peak in varved sediments from Nicolay Lake, Cornwall Island in the Arctic Ocean (Lamoureux, 1999) implies that insufficient

depth resolution and/or bioturbation may explain the absence of the Chernobyl peak in some of the aforementioned sites.

Significant levels of ^{137}Cs first appeared in the atmosphere in the early 1950s as a result of above ground nuclear weapons testing. The number of nuclear detonations reached its highest in 1962, resulting in a maximum in ^{137}Cs fallout the following year. As a consequence of the nuclear weapons Limited Test Ban Treaty instated in 1963 (Carter and Moghissi, 1977), little radioactive fallout was observed in the late 1960s and 1970s in the northern hemisphere. Because ^{137}Cs deposition reflects the history of nuclear tests, this artificial radionuclide is commonly used as a chronostratigraphic marker to constrain dating records (Anderson et al., 1988; Ritchie and McHenry, 1990; Spliethoff and Hemond, 1996; Appleby, 2001). Following the 1986 Chernobyl accident, the atmospheric concentration of ^{137}Cs in Europe remained ~4-times higher than the 1963 levels for several months (Cambray et al., 1987) and a number of investigations reported the presence of Chernobyl-derived ^{137}Cs in sediment traps from the Black Sea and a lake in Switzerland (Buesseler et al., 1987; Wieland et al., 1993) and in surficial sediments from Denmark (Ehlers et al., 1993), Netherlands (Zwolsman et al., 1993), Switzerland (Dominik and Span, 1992; Gunten et al., 1997; Albrecht et al., 1998) and UK (Gevao et al., 1997). At these locations, elevated activities of ^{137}Cs imply that the 1986 peak can serve as a valuable sedimentary marker for several decades (^{137}Cs half-life = 30.2 yr).

As part of a study to develop historical records of combustion (Lima et al., 2003), we collected sediment cores from an estuarine anoxic basin site in southern Rhode Island and generated detailed ^{210}Pb , ^{137}Cs , and varve chronologies. The anoxic nature of this environment inhibits bioturbation, creating undisturbed laminations that are ideal for sediment dating. Here, the varve chronology is used to validate the dates generated by ^{210}Pb models, and not the other way around. We revisit the ^{210}Pb models used for dating recent sediments and show that ^{137}Cs derived from the Chernobyl accident was

* Author to whom correspondence should be addressed (alima@whoi.edu).

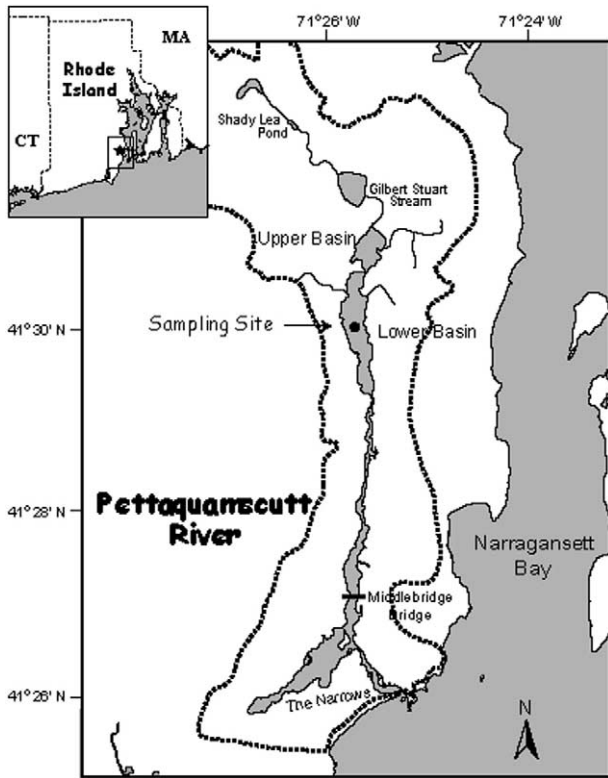


Fig. 1. Map showing the boundaries of the watershed of the Pettaquamscutt River (RI) (dotted line) and the location of the site of sediment freeze-core collection. Modified after Lima et al. (2003).

preserved in sediments from a site in the Northeastern United States.

2. EXPERIMENTAL

2.1. Study Area

The Pettaquamscutt River, also known as the Narrow River, is located in Washington County, southern Rhode Island (Fig. 1). This estuary is ~9.7 km long, ranges from 100 to 700 m in width (Boothroyd, 1991) and has a small (35 km²) drainage area (Orr and Gaines, 1973). The Pettaquamscutt can be morphologically divided into two basins and a channel. The upper basin is 13.5 m deep at its maximum and receives input of freshwater from the Gilbert Stuart Stream. The lower basin is deeper (19.5 m), has a larger area and is confined to the north by a shallow sill (less than 1 m deep) and to the south by a long narrow channel that connects it to its salt-water source, Rhode Island Sound. The bottom waters and sediments of the upper and lower basins are permanently anoxic, mostly due to a stable salinity-dominated stratification of the water column (Gaines and Pilson, 1972). As a result, no bioturbation of the surficial sediments is observed and annually laminated layers are well preserved (Fig. 2).

2.2. Sampling

Freeze-cores were collected in the deepest part of the lower basin (Fig. 1) in April 1999 (Lima et al., 2003). Unlike gravity coring, which can disturb the surficial sediments and lead to compaction of sediment layers, freeze coring allows for recovery of intact sediment-water interfaces (Shapiro, 1958). Consequently, this sampling technique is ideal for high-resolution records of aquatic sediments, and especially those containing high amounts of siliceous tests that render sediments flocculant (Koide et al., 1973). Before lowering into the water, the aluminum corer (30 × 8 × 165 cm) was filled with a slurry of dry ice

and methanol. The corer was lowered to approximately 2 m above the sediment-water interface, allowed to drop into the sediment and left there for ~10–15 min, so that a thick slab of sediment froze onto the metal surface of the corer. After collection, the sediment slabs were separated from the corer, wrapped in aluminum foil, kept in dry ice, and transported back to the laboratory where they were stored in a chest freezer (–18°C). X-radiographs of the frozen slabs collected in 1999 showed laminated sediments and confirmed the absence of benthic animal burrows (Fig. 2). Here, we report results from the slab that showed the most distinct and the highest number of laminations on the X-radiographs. It is noteworthy that the cores did not show different number of laminations, the X-radiographs did. When we were choosing the cores, we were not looking at thin-sections, but at X-radiographs taken at a medical facility. Because the X-ray machine was not dedicated to X-raying sediments and the cores varied in thickness, different numbers of laminations were observable in each core. However, the sand layers deposited by the 1954 and 1938 hurricanes were distinct in every X-ray slide.

Before sampling the core, a 10-cm-wide subsection of the slab was cut lengthwise to be made into thin sections for subsequent varve counting (²¹⁰Pb measurements and varve counting were conducted on the same sediment slab). The frozen sediment was subsequently sliced using a compact tile saw equipped with a diamond wafering blade, while the slab was kept frozen by regular applications of liquid nitrogen. The sediment-water interface was sectioned at 1 cm, while the remaining of the core was sliced at 0.5 cm intervals. The samples were placed in precombusted glass-jars, air-dried, homogenized with a mortar and pestle, and stored until radiometric measurements and geochemical analyses were performed. The deepest portion of the lower basin of the Pettaquamscutt River has been sampled repeatedly over the years. In this paper we also refer to data obtained for freeze-cores collected in 1987, 2000, and 2003.

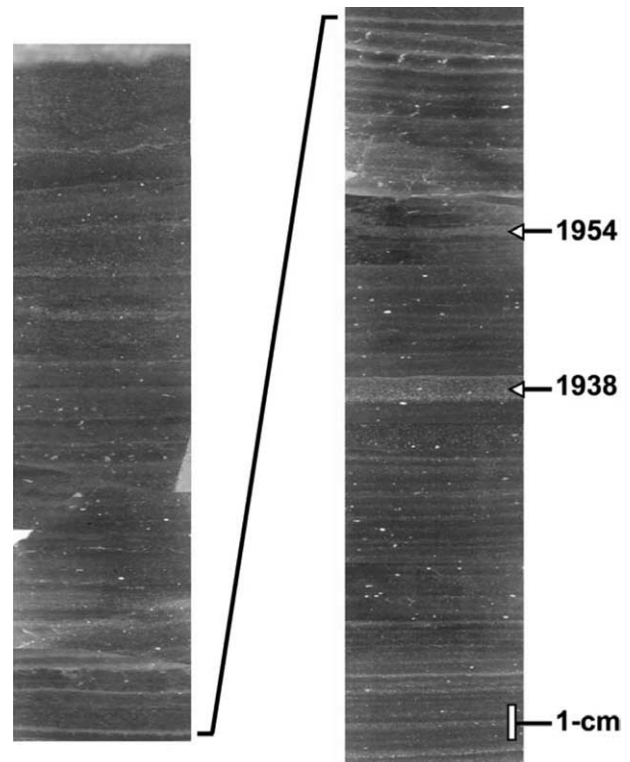


Fig. 2. Composite image of 20th century laminations from the lower basin of the Pettaquamscutt River. Laminae deposited by historical hurricanes (1954, 1938) are marked with arrows and help constrain the varve chronology. The width of the composite has been exaggerated 2×; scale bar = 1 cm.

2.3. Varve Counting

Sediment pieces (6 cm × 4 cm) were taken from a 10-cm wide subsection saved for varve counting, dehydrated and embedded with Spurr (1969) resin, following the procedure of Pike and Kemp (1996). The resulting slabs of sediment/resin were mounted on glass slides and thin-sectioned using standard petrographic techniques. Thin sections were scanned under cross-polarized films using a flat bed scanner with transparency capabilities to produce tag image file (TIFF) digital images with resolutions of 1440 dpi (De Keyser, 1999). The images were imported into Adobe Photoshop, lamination boundaries were marked with the “path” tool and the exported paths were processed using an algorithm that counts and measures the thickness of each lamination (Francus et al., 2002). Paths were constructed one or two times per thin section. In the cases where the counts were repeated, the varve numbers remained consistent (error within ~1%). Although only two counts per thin section limits the confidence of an individual count, we address this by counting numerous cores from the same location. By using this multiple core method, we can address both counting error as well as disturbances in individual core records. The resulting data files for each sediment piece were overlain to produce a continuous record of varve thickness, number, and depth. Because during core recovery the sides of the cores are broken off, the sediment close to the edge can have slight hiatuses at the breaks. To make sure our varve chronology was complete, we compiled data from freeze cores taken in 1999, 2000, and 2003 to produce a master varve chronology for the lower basin. Distinct sediment marker bands were used as a primary tool for correlation between cores. Using such laminae, the cores were divided into sections representing between 26 and 63 couplets. Sections from all cores were compared using skeleton plots of couplet thickness (Lamoureux, 2001). This technique was used to address poorly defined couplets in the original core. This multiple-core chronology is superior to that from a single core because it enables the identification of laminae that may have been disturbed in the original core (Lamoureux, 2001). In addition, we would like to emphasize that we were not using completely different cores for varve counting and ²¹⁰Pb measurements (although that is not uncommon in the literature).

2.4. Gamma Spectrometry

Aliquots of dry sediment (1–2 g) were measured for ²¹⁰Pb, ²²⁶Ra and ¹³⁷Cs by direct gamma counting using a high purity germanium detector (Canberra model GCW 4023S) with a closed-end coaxial well. ²¹⁰Pb was measured by its emission at 46.5 keV, and ²²⁶Ra by the 351 keV emission by its daughter isotope ²¹⁴Pb (with a correction for losses of the intermediary gaseous isotope ²²²Rn). Cesium-137 was measured by its emissions at 661 keV. Detector efficiency was determined by counting a National Institute of Standards and Technology (NIST) traceable mixed liquid gamma standard (Isotope Products Labs) and a certified ²¹⁰Pb standard (Physikalisch Technische Bundesanstalt [PTB]). The background corrected counts were then analyzed with the GESPECOR software, which uses Monte Carlo simulations to correct for self-absorption and coincidence-summing effects (Sima et al., 2001). Excess ²¹⁰Pb was calculated as the difference between the measured total ²¹⁰Pb and the estimate of the supported ²¹⁰Pb activity as given by ²¹⁴Pb (²¹⁰Pb_{exc} = ²¹⁰Pb_{total} – ²¹⁴Pb). Counting errors for ¹³⁷Cs ranged from 5.8 to 40% of the total activity (± 1σ) and those for ²¹⁰Pb_{total} and ²¹⁴Pb were propagated to ²¹⁰Pb_{exc}, which ranged between 4%–20% (± 1σ). Minimum detectable activity was calculated at 0.004 Bq for ¹³⁷Cs and 0.040 Bq for ²¹⁰Pb_{exc}.

2.5. Total Organic Carbon, Radiocarbon Content and Density Measurements

Dry sediment densities were measured at 2-cm intervals using a 2-mL specific gravity bottle (calibrated volume = 1.98-mL). Sediment densities were measured at odd numbered depths (1 cm, 3 cm, . . .). For all other sediment layers we decided against fitting the data, interpolating it or using a constant density value (which is how most calculations are done). Instead, we assumed that density did not change dramatically between measurements. Therefore, for middepth 2.25-cm we used the density value obtained for the layer above it (1 cm). This procedure was used throughout the core.

A Fisons 1108 elemental analyzer was used to measure the total organic carbon (TOC) content of the samples. To remove the inorganic fraction, ~2 mg of dry sample was weighed into a silver capsule and acidified with HCl under vacuum. The samples were then dried in an oven at 50°C, folded, placed inside tin capsules (for better catalysis of the oxidation reaction) and analyzed. Samples were run in triplicate and all reported weight percentages represent the mean ± one standard deviation. Carbon content was determined through a five-point calibration curve of a sulfanilamide standard (0.05 to 0.50 mgC). Subsamples of the dry sediment were submitted to the National Ocean Sciences Accelerator Mass Spectrometry (NOSAMS) facility where they were analyzed for radiocarbon (¹⁴C) and stable carbon isotopic composition (δ¹³C¹) according to established procedures (McNichol et al., 1994). ¹⁴C values are expressed as Δ¹⁴C², which is the measured ¹⁴C concentration normalized to preindustrial atmospheric values reported in permil (‰) (Stuiver and Polach, 1977). Routine precision for δ¹³C and Δ¹⁴C measurements at NOSAMS are ~0.1 and 5‰, respectively.

3. ²¹⁰Pb AGE MODELLING

Since its introduction in the early 1970s, the use of ²¹⁰Pb as a dating technique has become established as an important means of deriving sedimentation rates and ages of recently deposited sediments. Lead-210 enters aquatic systems by direct precipitation or by run-off from the catchment area. The total amount of ²¹⁰Pb present in lake sediments represents a mixture of that formed within the sediment from the decay of ²²⁶Ra deposited by soil erosion (supported ²¹⁰Pb), and that formed in the atmosphere by the decay of ²²²Rn (unsupported or excess ²¹⁰Pb, ²¹⁰Pb_{exc}). The activity of supported ²¹⁰Pb is estimated by measuring the activity of either ²¹⁴Pb or ²²⁶Ra, while the activity of ²¹⁰Pb_{exc} is determined by the difference between the total and the supported ²¹⁰Pb (²¹⁰Pb_{exc} = ²¹⁰Pb_{total} – ²¹⁴Pb). The decay of this atmospherically derived ²¹⁰Pb provides a measure of the rate of deposition of the sediment column. In the absence of sediment mixing, two models are commonly used to derive age-depth correlations in sedimentary profiles. The constant rate of supply (CRS) model (Appleby and Oldfield, 1978) assumes that sedimentation rate and sediment compaction change throughout the core and automatically corrects for these parameters, while the constant initial concentration (CIC) model (Goldberg, 1962; Krishnaswamy et al., 1971) assumes that sedimentation rate is constant in the area under study and requires that the depth of the sediment column be corrected for compaction before the method be applied. Both models assume no postdepositional migration of ²¹⁰Pb and a constant flux of ²¹⁰Pb_{exc} at the sediment-water interface.

Concentration and flux relate to each other by the equation

$$C = \frac{F}{r} \quad (1)$$

where r is the mass accumulation rate. By assuming a constant flux of ²¹⁰Pb_{exc} at the sediment-water interface and constant sedimentation rate, the CIC model fixes the concentration of ²¹⁰Pb_{exc} at the surface. If no physical processes alter the amount of ²¹⁰Pb_{exc} in the surface sediments, the activity of ²¹⁰Pb_{exc} declines down the sedimentary profile according to its natural radioactive decay:

$$C(x) = C_{(0)} \exp(-\lambda t) \quad (2)$$

where C is the ²¹⁰Pb_{exc} concentration per mass of dry sediment (Bq kg⁻¹) at the sediment-water interface ($C_{(0)}$) and at depth x ($C(x)$), λ is the decay constant of ²¹⁰Pb (0.03114 yr⁻¹), and t is the age of the sediment at depth x . Because the age of the sediment is a function of sedimentation rate (R) (cm yr⁻¹) and depth (x) (cm), Eqn. 2 takes the form:

$$C(x) = C_{(0)} * \exp\left(-\frac{\lambda}{R} * x\right) \quad (3)$$

¹ $\delta^{13}C(\text{‰}) = \left\{ \left[\frac{{}^{13}C}{{}^{12}C} \right]_{\text{sample}} / \left[\frac{{}^{13}C}{{}^{12}C} \right]_{\text{PDB}} - 1 \right\} \times 1000$; where PDB = Pee Dee Belemnite carbonate standard.

² $\Delta^{14}C(\text{‰}) = (\% \text{modern} \times e^{-\lambda t} - 1) \times 1000$, where λ = ¹⁴C decay constant and t = calendar age.

From this point, there are at least three different ways of calculating sedimentation rate using the CIC model. Graphically, the semilogarithmic plot of $^{210}\text{Pb}_{\text{exc}}$ concentration against depth is predominantly linear and the mean sedimentation rate is taken from the ratio of the decay constant of ^{210}Pb to the slope of the line (CIC with no compaction correction and constant sedimentation rate). If compaction plays an important role in the study site, such as in the Pettaquamscutt River sediments, the slope of this line decreases towards the top of the core as a result of reduced compaction at surface, assuming no physical mixing and no change in accumulation rate has taken place. The effects of compaction can be eliminated from the CIC model by expressing depth in terms of cumulative dry mass of sediment (m) (g cm^{-2}):

$$\text{Dry bulk density (DBD)}_{(x)} = (1 - \phi_{(x)})\rho_{\text{sed}} \quad (4)$$

$$m = \sum (\text{DBD}_{(x)} \times T_{(x)}) \quad (5)$$

where $\phi_{(x)}$ is the porosity at depth x ; ρ_{sed} is the density of the sediment at depth x and T is the thickness of the sediment layer. Eqn. 3 now takes the form (Hughen et al., 1996):

$$C_{(x)} = C_{(0)} * \exp\left(-\frac{\lambda}{r} m\right) \quad (6)$$

r , the mass accumulation rate ($\text{g cm}^{-2} \text{y}^{-1}$), is calculated by the ratio of the decay constant of ^{210}Pb to the slope of the line of the semilogarithmic plot of $^{210}\text{Pb}_{\text{exc}}$ concentration against cumulative dry mass, and sedimentation rate (R) as a function of depth is calculated by (Hughen et al., 1996) (CIC with compaction correction):

$$R = \frac{r}{(1 - \phi)\rho_{\text{sed}}} \quad (7)$$

A third way of calculating sedimentation rate with the CIC model is by simply applying Eqn. 2 to the data (CIC with no compaction correction and variable sedimentation rate). Since $C_{(0)}$ is the $^{210}\text{Pb}_{\text{exc}}$ concentration per mass of dry sediment (Bq kg^{-1}) at the sediment-water interface and $C_{(x)}$ is the $^{210}\text{Pb}_{\text{exc}}$ concentration of the layer under investigation, then t , the age of the sediment at depth x , can be calculated for each depth. Because this method does not fit a regression line through the data, calculated sedimentation rates vary with depth and yield scattered results.

In the CRS model, the initial concentration of $^{210}\text{Pb}_{\text{exc}}$ and the sediment accumulation rate vary with time, but their product remains constant and equals the flux of $^{210}\text{Pb}_{\text{exc}}$ that reaches the sediment-water interface. The constant flux assumption implies a constant residue of $^{210}\text{Pb}_{\text{exc}}$ within the sediment column. Eqn. 2 then takes the form:

$$A_{(x)} = A_{(0)}\exp(-\lambda t) \quad (8)$$

where $A_{(x)}$ is the residual $^{210}\text{Pb}_{\text{exc}}$ in the core below depth x (Bq m^{-2}), and $A_{(0)}$ is the entire $^{210}\text{Pb}_{\text{exc}}$ inventory below the sediment-water interface. Because measurements are rarely made on every sample from a core, the midpoint procedure is applied in most cases. The residual $^{210}\text{Pb}_{\text{exc}}$ for each sediment layer is calculated by multiplying $^{210}\text{Pb}_{\text{exc}}$ concentration ($C_{(x)}$) by cumulative dry mass (m), using the trapezium rule described by Appleby (2001). The age of each sediment layer can be calculated by rearranging Eqn. 8,

$$t = \frac{1}{\lambda} \ln\left(\frac{A_{(0)}}{A_{(x)}}\right) \quad (9)$$

and the mass accumulation rate at time t from (Appleby, 2001)

$$r = \frac{\lambda A_{(x)}}{C_{(x)}} \quad (10)$$

For a more extensive discussion of applications of CIC and CRS models and derivation of mathematical equations, refer to Appleby (2001), Turner and Delorme (1996), and Eakins (1983).

4. RESULTS AND DISCUSSION

4.1. Sediment Properties

Water content, density and porosity are some of the basic parameters necessary for dating sediments. Most studies assume a sediment dry density between 2.3 and 2.7 g cm^{-3} throughout a core. However, measured dry densities for the Pettaquamscutt River sediments ranged from 1.58 to 2.29 g cm^{-3} (Table 1), well below the commonly assumed values. These low values reflect the composition of the sediments, which are dominated by diatom frustules (45 to 65%) and organic matter, with small amounts of pyrite and clastic material and no carbonates (Orr and Gaines, 1973). The organic carbon content varied from an average of $8.1 \pm 0.7\%$ in surface layers to $9.8 \pm 0.8\%$ below 30 cm, and increases in organic carbon content were frequently associated with declines in sediment density.

Porosity (ϕ) was calculated from the weight percent of water in the sediments, following the equation by Berner et al. (1971):

$$\phi = \frac{W \times \rho_{\text{sed}}}{W \times \rho_{\text{sed}} + (1 - W)\rho_{\text{water}}} \quad (11)$$

where W is the weight percent water, ρ_{sed} is the dry density of the sediment, and ρ_{water} is the density of the pore water ($\rho_{\text{water}} = 0.9997$; assuming a salinity of 27 ‰ and temperature of 10°C for the pore water (O'Sullivan et al., 1997). The porosity in the Pettaquamscutt River sediments ranged from 0.965 at the surface to an average of 0.883 below 30 cm (Table 1). Although this is only a 8.5% decrease over 30 cm, the ratio of solid to pore-water volume $[(1 - \phi)/\phi]$ increases by almost a factor of 3. This variation indicates that the bottom layers of the core are undergoing continuous compaction due to the weight of overlying sediments, so that the thickness of a 1-yr increment is larger at the surface than in deeper layers (Fig. 2).

4.2. Varve Counting and ^{210}Pb Chronology

A key assumption in varve counting chronologies is that two seasonally controlled laminae are deposited annually and sediment ages can be calculated by counting each couplet. A predominantly biogenic layer forms as phytoplankton remains from the spring/summer bloom settle out of the water column. This biogenic layer appears dark under cross-polarized light due to the small amounts of birefringent minerals. During the fall/winter productivity is much lower and clastic material from the watershed dominates the input to the sediment surface. This clastic layer appears bright under cross-polarized light. Examination of the thin sections from the upper sediment column of the lower basin of the Pettaquamscutt River showed that this pattern of deposition was present in the sediments, allowing a precise varve chronology. Additional constraints to the varve chronology come from occasional coarse-grained (fine sand) winter laminae. These layers are deposited as large hurricanes rework the material from the surrounding watershed. The good correlation between coarse-grained layers and the two largest hurricanes to hit Rhode Island in the twentieth century (1954, 1938, Fig. 2, Table 2) supports the accuracy of this varve chronology.

Table 1. Values obtained for selected sediment properties, radiometric determinations, ²¹⁰Pb chronology calculation using the CRS model and varve chronology are listed below.

Midpoint depth (cm)	ρ_{sed} (g cm ⁻³)	W (%)	Porosity ϕ	DBD (g cm ⁻³)	m (g cm ⁻²)	²¹⁰ Pb _{exc} (Bq kg ⁻¹)	¹³⁷ Cs (Bq kg ⁻¹)	CRS model date	Varve date
0.5	2.3	93	0.9668	0.076	0.04	551 ± 23	≤ DL ^a	1999 ± 0	1998
2.25	2.3	92	0.9607	0.090	0.18	440 ± 29	≤ DL	1995 ± 1	1996
4.25	2.2	91	0.9551	0.099	0.37	371 ± 22	≤ DL	1992 ± 1	1993
5.25	1.9	90	0.9434	0.109	0.48	473 ± 28	≤ DL	1990 ± 1	1991
6.25	1.9	89	0.9386	0.118	0.59	282 ± 13	3 ± 1	1988 ± 1	1989
7.25	2.0	88	0.9325	0.135	0.72	375 ± 27	6 ± 1	1987 ± 1	1987
8.25	2.0	87	0.9429	0.114	0.84	310 ± 25	5 ± 2	1985 ± 2	1985
10.25	2.1	88	0.9350	0.135	1.09	302 ± 30	≤ DL	1981 ± 2	1981
12.25	1.9	88	0.9243	0.148	1.37	217 ± 15	≤ DL	1977 ± 2	1976
14.25	1.9	87	0.9222	0.152	1.67	220 ± 23	11 ± 2	1972 ± 2	1972
16.25	1.9	87	0.9263	0.143	1.97	179 ± 12	16 ± 2	1968 ± 2	1968
17.25	1.9	86	0.9222	0.150	2.11	195 ± 11	21 ± 2	1966 ± 2	1965
18.25	1.9	86	0.9120	0.170	2.27	158 ± 15	25 ± 2	1963 ± 2	1962
19.25	1.9	85	0.9119	0.169	2.44	135 ± 9	14 ± 2	1961 ± 3	1960
20.25	1.9	85	0.8984	0.195	2.63	149 ± 10	11 ± 1	1958 ± 3	1957
22.25	2.0	84	0.9132	0.174	2.99	112 ± 11	4 ± 1	1953 ± 3	1950
24.25	2.0	85	0.9155	0.166	3.33	125 ± 8	≤ DL	1947 ± 3	1944
26.25	2.0	84	0.9095	0.177	3.68	93 ± 11	≤ DL	1941 ± 4	1937
30.25	1.7	84	0.8953	0.183	4.40	96 ± 16	≤ DL	1926 ± 4	1920
34.25	1.8	83	0.8930	0.194	5.15	47 ± 9	≤ DL	1904 ± 5	1904
38.25	1.7	82	0.8841	0.195	5.93	23 ± 7	≤ DL	1882 ± 5	1988
42.25	1.8	82	0.8744	0.221	6.76	8 ± 3	≤ DL	1863 ± 6	1871
44.25	1.7	81	0.8827	0.199	7.18	7 ± 3	≤ DL	1855 ± 7	1863
46.25	1.6	82	0.8785	0.193	7.58	-3	≤ DL		1856
48.25	1.6	81	0.8715	0.203	7.97	-5	≤ DL		1845
49.25									1841

^a DL = detection limit = 0.004 Bq.

Radiometric results obtained for the Pettaquamscutt River sediments are shown in Figure 3 to 6 and Table 1. The down-core profile of ²¹⁴Pb activities is nearly uniform with depth, while total ²¹⁰Pb activities decrease exponentially until ²¹⁴Pb-supported levels are reached at ~42 cm (Fig. 3a). The resulting ²¹⁰Pb_{exc} profile (Fig. 3b) follows closely the exponential shape of ²¹⁰Pb_{total}, attesting to the good preservation of these sediments. Indeed, if the surficial sediments were physically disturbed (either during recovery of the core or due to rapid bioturbation), the ²¹⁰Pb_{exc} distribution would be uniform within the mixed layer.

Discrepancies among the three different methods for CIC calculation and the CRS model were checked against independent varve counting (Fig. 4, Table 2). The different ways of determining age-depth correlations using the CIC model yield contrasting results. Compaction is an important process in the sediments of the Pettaquamscutt River, consequently the CIC

chronologies generated by neglecting compaction (e.g., calculating age from the slope of the plot of ²¹⁰Pb_{exc} concentration against depth and from Eqn. 2 did not agree well with the varve counts. The constant sedimentation rate calculated using the slope of the plot of ²¹⁰Pb_{exc} concentration against depth overestimated sedimentation rates for layers above 30 cm resulting in ages older than the varve chronology (Table 2), while the CIC model with no compaction correction and variable sedimentation rate resulted in scattered values. The CIC model that corrects for compaction of the sediment layers (e.g., from the slope of the plot of ²¹⁰Pb_{exc} concentration against cumulative dry mass) yielded ages slightly older than those from the CRS (Table 2), probably because this CIC model does not account for the possibility of small changes in mass accumulation rate. For instance, sediments deposited at the peak of ¹³⁷Cs deposition (18.25 cm) were assigned a date of 1958 by this CIC model and 1963 by the CRS model (Table 2), the latter date being in

Table 2. Date of deposition obtained for key horizons using the three variations of the CIC model, the CRS model and varve counting.

Depth (cm)	CIC	CIC	CIC	CRS	Varves	Comment
	no compaction constant R^a	no compaction variable R^a	compaction correction			
7.25	1979 ± 1	1986 ± 1	1986 ± 1	1987 ± 1	1987	Chernobyl peak
18.25	1948 ± 3	1958 ± 3	1958 ± 2	1963 ± 2	1962	Maximum fallout
21.0 ^b	1940 ± 4 ^b	1953 ± 4 ^b	1949 ± 3 ^b	1956 ± 3 ^b	1954	1954 Hurricane—sand layer
25.8 ^b	1926 ± 4 ^b	1943 ± 4 ^b	1935 ± 4 ^b	1943 ± 4 ^b	1938	1938 Hurricane—sand layer

^a Sedimentation rate.

^b Interpolated date of deposition.

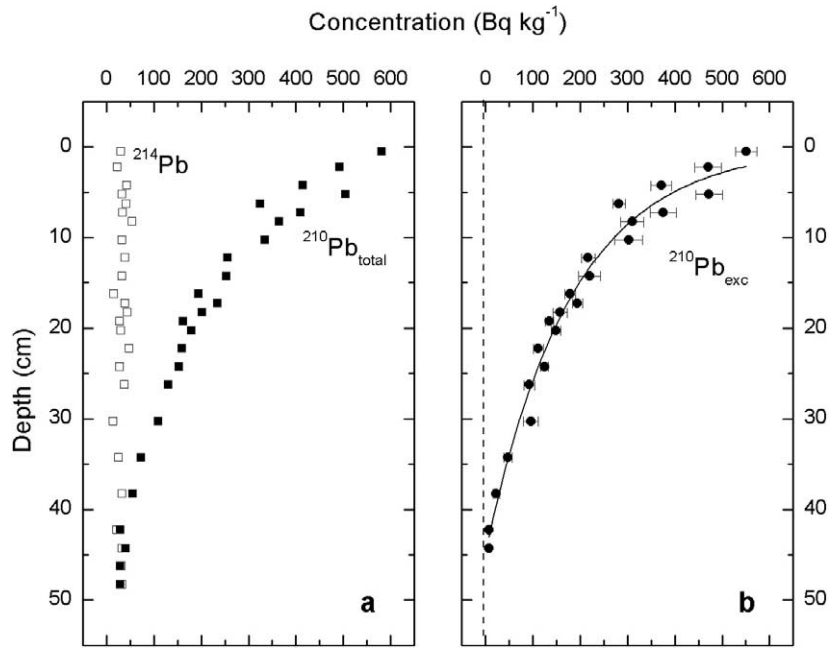


Fig. 3. (a) Downcore profile of ²¹⁴Pb activities is nearly uniform with depth, while total ²¹⁰Pb activities decrease exponentially until supported levels are reached at 42 cm. (b) Resulting ²¹⁰Pb_{exc} profile (exponential fit) is consistent with the lack of rapid bioturbation of the sediments.

good agreement with the historical fallout of ¹³⁷Cs. If the sedimentation rate at the Pettaquamscutt River were constant, then both ²¹⁰Pb models would have produced identical results. Instead, the results obtained by the CRS model followed the varve chronology more closely than the CIC model that corrects for compaction of the sediment layers, as expected for an environment that has undergone changes in sedimentation rate.

Land use changes within a watershed tend to modify the rate of sediment transport to nearby lakes and rivers. In 1995, only 22.7% of the watershed of the Pettaquamscutt River was comprised of residential land (Hubeny and King, 2003). Even though there are no recent estimates available for land use for residential purpose, this percentage is likely to have increased in the past decade due to new urban developments in the region.

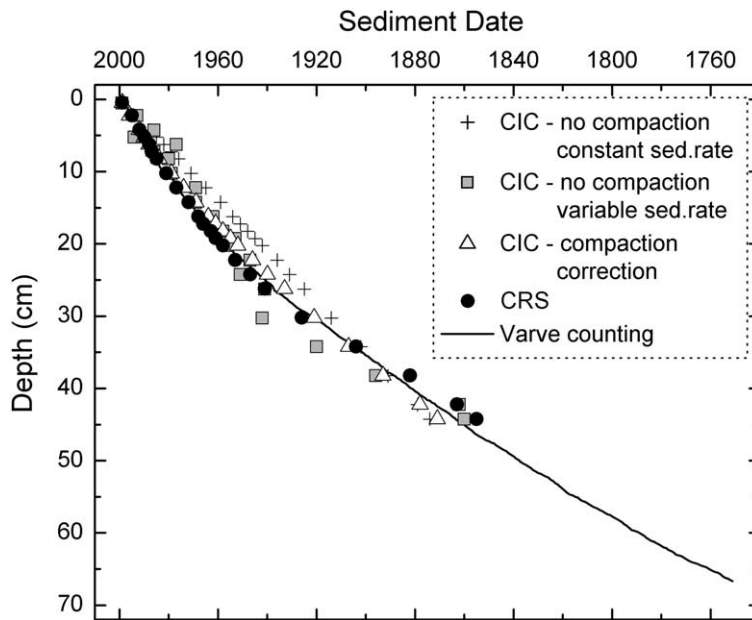


Fig. 4. Chronology results obtained by the CRS model and by three different forms of applying the CIC model were checked against the independent varve counting.

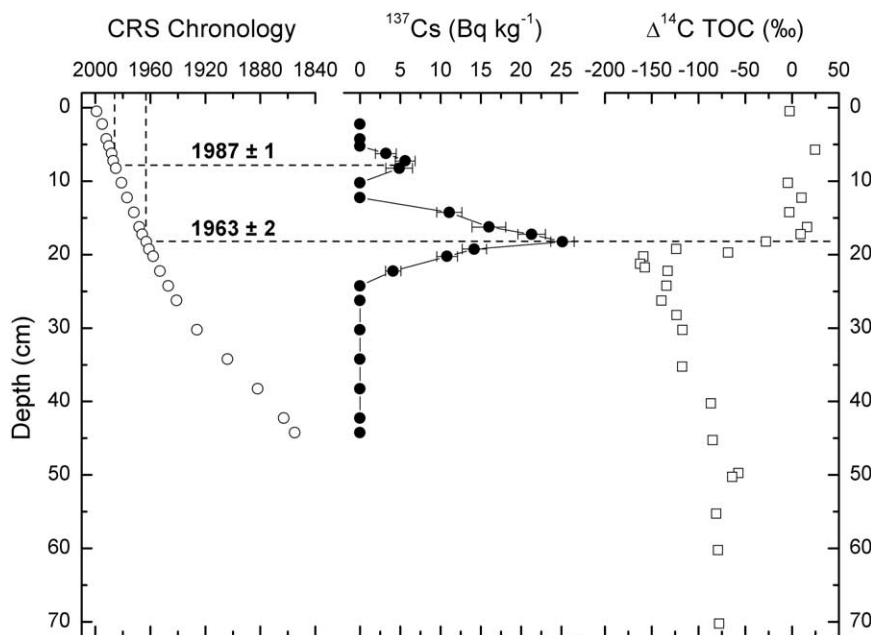


Fig. 5. Radioactivity released by nuclear bomb testing in the 1960s was preserved in the Pettaquamscutt River sedimentary record in the form of a sharp ^{137}Cs peak and increased amounts of radiocarbon in the total organic carbon ($\Delta^{14}\text{C}$ TOC). A smaller and more surficial peak in ^{137}Cs activity dated of 1987 is consistent with fallout resulting from the Chernobyl accident.

Varve counting results were also used as an independent chronology that helped us evaluate the different ^{210}Pb models. The good age agreement obtained between the varve counts and ^{210}Pb dates calculated by the CRS model (e.g., within 1 yr at 1960 and within 8 yr at 1860, Fig. 4, Table 2) validated this dating technique for the upper 35-cm of the Pettaquamscutt River sedimentary column. We could have used the varve chronology alone to date the sediments of the Pettaquamscutt River, however our goal was to apply the ^{210}Pb technique to date recent sediments and use varve counting to extend the chronology beyond the limit of the ^{210}Pb method (100–150 yr). Therefore, CRS model ages were used to date the uppermost 34-cm of the sediment column, while the varve chronology was applied for sediment horizons between 35 and 70 cm. The use of varve counts instead of the CRS model in the top 34-cm of the core would not have changed the age estimates significantly (Table 1).

4.3. ^{137}Cs and ^{14}C Profiles

The sedimentary profile of ^{137}Cs (Fig. 5) in the Pettaquamscutt River shows good correlation with the history of atmospheric deposition of radionuclides derived from nuclear weapons testing. The first detection of ^{137}Cs in the sediment core (22.25 cm) corresponds to 1953, which closely matches the early 1950s increase in total fission yields from the explosions (Carter and Moghissi, 1977). The yield and number of nuclear detonations per year peaked in 1962, resulting in extensive deposition of radionuclides in the Northern Hemisphere in 1963, the year the nuclear weapons Limited Test Ban Treaty was signed (Carter and Moghissi, 1977; Appleby, 2001). The elevated amounts of radioactivity released in the 1960s were

preserved in the Pettaquamscutt River sedimentary record in the form of a sharp ^{137}Cs subsurface maximum with highest activity in sediments with an assigned deposition age of 1963, as well as increased amounts of radiocarbon (^{14}C) in the total organic carbon (TOC) (Fig. 5). Nuclear weapons tests roughly doubled the levels of ^{14}C in the atmosphere (Levin and Kromer, 1997), raising the $\Delta^{14}\text{C}$ of CO_2 to values greater than +900 permil (‰) (Levin et al., 1985), the so-called “bomb spike.” The incorporation of bomb- ^{14}C into terrestrial and aquatic plant biomass through photosynthetic carbon fixation is manifested in the sedimentary record as an increase in $\Delta^{14}\text{C}$ in the TOC (Fig. 5). The relative timing of the ^{137}Cs peak and the rapid $\Delta^{14}\text{C}$ rise is primarily determined by the pathways by which these radionuclides are incorporated into the sediments. Cesium-137 deposited on aquatic systems by direct dry and wet fallout quickly sorbs onto settling particles, reaching the sediments in a matter of months (depending on the water column depth) (Santschi et al., 1988; Wieland et al., 1993). The rate at which atmospheric ^{14}C signals propagate into sedimentary TOC depends on the relative contributions from different organic carbon sources (e.g., terrestrial vs. marine) and the residence times for carbon in each reservoir. The similar timing in the rise in $\Delta^{14}\text{C}$ and ^{137}Cs (Fig. 5), together with the relatively depleted stable carbon isotopic composition ($\delta^{13}\text{C}$) of the TOC throughout the core ($-24.1 \pm 0.5\text{‰}$, $n = 37$) suggests that terrestrial OC plays a significant role in the amount of “pre-aged” organic carbon deposited in the Pettaquamscutt River sediments. However, the fact that the $\Delta^{14}\text{C}$ profile of TOC does not exceed 0‰, typical of atmospheric “bomb ^{14}C ” (Levin and Hesseshaimer, 2000), implies that recent material is being diluted by relict terrestrial OC from sedimentary and fossil sources.

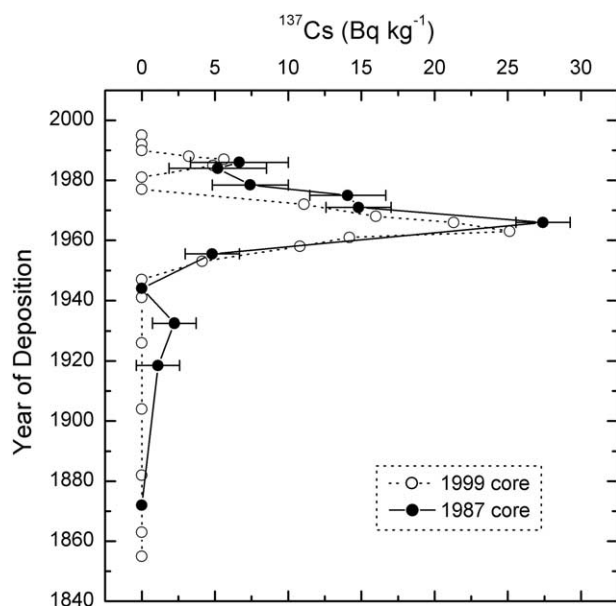


Fig. 6. The ^{137}Cs profile obtained for a core collected in 1987 in the Pettaquamscutt River (Appleby, 1993) showed a rise in activity that correlates extremely well with the Chernobyl ^{137}Cs maximum observed in this study.

The downcore profile of ^{137}Cs also reveals a smaller peak in activity closer to the surface ^{210}Pb -dated at 1987. The timing of this peak is consistent with fallout resulting from the release of radioactivity that followed the 1986 Chernobyl reactor fire in Ukraine. Elevated surface air concentrations and ground deposition of radionuclides due to the Chernobyl accident were reported throughout the Northern Hemisphere, in locations as far apart as Japan (Aoyama et al., 1986), Switzerland (Santschi et al., 1988), and Sweden (Devell et al., 1986). At some European sites, the deposition of Chernobyl ^{137}Cs provided another datable horizon in the sediments, characterized in some cases by an even greater inventory than that resulting from the bomb tests (Dominik and Span, 1992; Ehlers et al., 1993; Callway et al., 1996; Gevao et al., 1997). Several studies reported the passage of the Chernobyl plume over the United States (Bondietti and Brantley, 1986; Larsen et al., 1986; Dibb and Rice, 1988; Feely et al., 1988). Surface air measurements conducted by the Environmental Measurements Laboratory (EML) following the announcement of the reactor explosion revealed simultaneous appearance of elevated radioactivity in both the eastern and western United States (Larsen et al., 1986). Monitoring of ^{137}Cs concentrations from 6 May to 29 May showed comparable surface air concentrations at 8 sites (Larsen et al., 1986), suggesting that the portion of the Chernobyl plume that arrived in the United States was homogeneous in composition. The closest EML monitoring sites to the Pettaquamscutt River were New York City (NY) and Chester (NJ). The total fallout of ^{137}Cs at these locations in May 1986 was $\sim 41 \text{ Bq m}^{-2}$ and $\sim 68.5 \text{ Bq m}^{-2}$, respectively and rainfall was responsible for $\sim 90\%$ of the deposition (Larsen et al., 1986). The higher efficiency of rain events in removing ^{137}Cs from the atmosphere relative to dry fallout was also demonstrated by ^{137}Cs accumulation rate measurements in Switzerland (70%–80% efficiency for rain vs. 20%–25% for dry fallout) (Santschi

et al., 1988), where the amount of ^{137}Cs deposited varied by at least one order of magnitude depending on the volume of precipitation (Dominik and Span, 1992). Because rain removes ^{137}Cs efficiently from the atmosphere, the ratio of ^{137}Cs deposited by wet fallout to the amount of precipitation that fell in May 1986 is fairly similar in both New York City ($12,440 \text{ Bq m}^{-3}$) and Chester ($13,880 \text{ Bq m}^{-3}$). To our knowledge there is no data on the surface air concentration or deposition of ^{137}Cs available for the state of Rhode Island following the Chernobyl accident. However, it is possible to estimate the total amount of ^{137}Cs deposited in the Pettaquamscutt River using the volumetric concentrations of ^{137}Cs calculated for New York and Chester and the amount of rain that fell in the Kingston area (RI) in May (4.77 cm ; NOAA, 1986). While this exercise gives a range in ^{137}Cs accumulation between 59.4 Bq m^{-2} and 66.2 Bq m^{-2} , the decay-corrected Chernobyl ^{137}Cs inventory in the Pettaquamscutt River sediments is only 22.5 Bq m^{-2} . Therefore, even if only a third of the Chernobyl ^{137}Cs washed out by local rain reached the sediments of the lower basin of the Pettaquamscutt River, the undisturbed nature of this depositional environment was able to record it.

Another line of evidence in support for the Chernobyl origin of the surficial ^{137}Cs peak derives from a freeze-core collected in 1987 in the lower basin of the Pettaquamscutt River (Fig. 6). After slicing the sediment at 2 cm intervals, ^{137}Cs , ^{210}Pb and ^{214}Pb were measured by direct gamma assay and chronology was calculated at the Liverpool University Environmental Radioactivity Research Center (Appleby, 1993). The down core profile of ^{137}Cs obtained for the 1987 core shows an increase in activity at 1 cm that correlates well with the Chernobyl ^{137}Cs maximum that we observed in this study. Deposition of ^{137}Cs derived from Chernobyl was not yet complete when the 1987 core was collected, which is reasonable considering that settling particles can reside in the water column for months before reaching the sediments (Santschi et al., 1988). However, the good agreement between cores collected 11 yr apart strengthens our belief that the elevated ^{137}Cs activities observed in the Pettaquamscutt River sediments at depths dated ~ 1987 record the deposition of Chernobyl ^{137}Cs in North American sediments. This peak in ^{137}Cs may not be recognizable in other locations of the United States possibly due to insufficient depth resolution of the cores, bioturbation of sediment layers or to the strong dependency of the fallout on local rainfall. The similarity of profile shapes for the 1987 and 1998 cores also indicates that diffusion and resuspension of ^{137}Cs are not significant in this system. If resuspension were a substantial process in the Pettaquamscutt River, higher ^{137}Cs activities would be observed at sediment layers younger than the maximum deposition (1963 and 1987). Furthermore, if diffusion were an active process, ^{137}Cs deposited in 1963 would have diffused into adjacent layers of lower activity and Figure 6 shows that this is not the case. Moreover, our density and porosity measurements show no evidence of a change in sediment morphology that could be connected with an interruption of the 1960s ^{137}Cs peak by a turbidite or other sandy layer. The presence of two ^{137}Cs marker points (1963 and 1987) in the Pettaquamscutt River segregates a portion of the sediment column that could prove valuable in the understanding of processes of decomposition and preservation of terrestrial and aquatic organic matter. This information is often lacking and can be useful in deter-

mining long-term diagenetic processes. Although the 1987 ^{137}Cs peak has low activity, it should still be detectable in this environment for the next few decades.

5. CONCLUSIONS

The anoxic and laminated sediments of the Pettaquamscutt River display the first known record of a Chernobyl ^{137}Cs peak in sediments from North America. The Chernobyl ^{137}Cs activities measured in the sediments are three-times lower than the calculated wet deposition for this area, demonstrating that rainfall alone could have produced the observed peak in ^{137}Cs . Although this peak may only be detectable for the next few decades, the presence of two ^{137}Cs marker points (1963 and 1987) identifies a segment of the sediment column that can potentially be used to evaluate the importance of compaction and decomposition and preservation of organic matter. Different methods for calculating the ^{210}Pb chronology were also evaluated in this study and checked against independent varve counting. In the case of the Pettaquamscutt River system, the CRS model provided results that matched the varve counting more closely and was applied for the most recent portion (100 yr) of the core. The absence of sediment mixing by benthic organisms was consistent with the exponentially decreasing trend of the $^{210}\text{Pb}_{\text{exc}}$ profile, making this site well suited for reconstruction of historical records.

Acknowledgments—We wish to thank J. Andrews (WHOI) for performing the ^{210}Pb and ^{137}Cs measurements, P. G. Appleby (University of Liverpool) for his invaluable help generating the ^{210}Pb chronology and J. Overpeck (University of Arizona), W. Wheeler (Stanford), and P. Francus (Université du Québec) for expertise on thin section preparation and varve analysis. The manuscript was greatly improved by comments from K. Buesseler (WHOI), J. Crusius (USGS) and three anonymous reviewers. This work was supported by funds from the National Science Foundation (OCE-9709478 and CHE-889172), and A. L. Lima acknowledges fellowship from the Brazilian Council for Research (CNPq). This is WHOI contribution No. 11321.

Associate editor: K. K. Falkner

REFERENCES

- Albrecht A., Reiser R., Lück A., Stoll J.-M. A., and Giger W. (1998) Radiocesium dating of sediments from lakes and reservoirs of different hydrological regimes. *Environ. Sci. Technol.* **32**, 1882–1887.
- Anderson R., Bopp R., Buesseler K., and Biscaye P. (1988) Mixing of particles and organic constituents in sediments from the continental shelf and slope off Cape Cod: SEEP-I results. *Cont. Shelf Res.* **8**, 925–946.
- Appleby P. G. (1993) *Radiometric Dating of Narragansett Bay Sediments*. University of Liverpool.
- Appleby P. G. (2001) Chronostratigraphic techniques in recent sediments. In *Tracking Environmental Change Using Lake Sediments*, Vol. 1 (eds. W. Last and J. Smol), pp. 171–203. Kluwer.
- Appleby P. and Oldfield F. (1978) The calculation of lead-210 dates assuming a constant rate of supply of unsupported ^{210}Pb to the sediment. *Catena* **5**, 1–8.
- ApSimon H. and Wilson J. (1986) Tracking the cloud from Chernobyl. *New Sci.* **1517**, 42–45.
- Ayoama M., Hirose K., Suzuki Y., Inoue H., and Sugimura Y. (1986) High level radioactive nuclides in Japan in May. *Nature* **321**, 819–820.
- Berner R. (1971) Diagenetic processes. In *Principles of Chemical Sedimentology* (ed. F. Press), pp. 86–113. McGraw-Hill.
- Bondiotti E. and Brantley J. (1986) Characteristics of Chernobyl radioactivity in Tennessee. *Nature* **322**, 313–314.
- Boothroyd J. (1991) The geologic history of Narrow River. *Maritimes* **35**, 3–5.
- Buesseler K., Livingston H., Honjo S., Hay B., Manganini S., Degens E., Ittekkot V., Izdar E., and Konuk T. (1987) Chernobyl radionuclides in a Black Sea sediment trap. *Nature* **329**, 825–828.
- Callway J., DeLaune R., and Patrick W. J. (1996) Chernobyl ^{137}Cs used to determine sediment accretion rates at selected northern European coastal wetlands. *Limnol. Oceanogr.* **41**, 444–450.
- Cambay R., Cawse P., Garland J., Gibson J., Johnson P., Lewis G., Newton D., Salmon L., and Wade B. (1987) Observations on radioactivity from the Chernobyl accident. *Nucl. Energy* **26**, 77–101.
- Carter M. and Moghissi A. (1977) Three decades of nuclear testing. *Health Phys. Press* **33**, 55–71.
- De Keyser T. L. (1999) Digital scanning of thin sections and peels. *J. Sediment. Res.* **69**, 962–964.
- Devell L., Tovedal H., Bergström U., Appelgren A., Chyessler J., and Andersson L. (1986) Initial observations of fallout from the reactor accident at Chernobyl. *Nature* **321**, 192–193.
- Dibb J. and Rice D. (1988) Chernobyl fallout in the Chesapeake Bay region. *J. Environ. Radioact.* **7**, 193–196.
- Dominik J. and Span D. (1992) The fate of Chernobyl ^{137}Cs in Lake Lugano. *Aquat. Sci.* **54**, 238–254.
- Eakins J. (1983) The ^{210}Pb technique for dating sediments and some applications. In *Radioisotopes in Sediment Studies*, pp. 31–47. IAEA-TecDoc 298, Vienna.
- Ehlers J., Nagorny K., Schmidt P., Stieve B., and Zietlow K. (1993) Storm surge deposits in North Sea salt marshes dated by ^{134}Cs and ^{137}Cs determination. *J. Coastal Res.* **9**, 698–701.
- Feely H., Helfer I., Juzdan Z., Klusek C., Larsen R. J., Leifer R., and Sanderson C. G. (1988) Fallout in the New York metropolitan area following the Chernobyl accident. *J. Environ. Radioact.* **7**, 177–191.
- Francus P., Keimig F., and Besonen M. (2002) An algorithm to aid varve counting and measurement from thin-sections. *J. Paleolimnol.* **28**, 283–286.
- Fuller C., Van Geen A., Baskaran M., and Anima R. (1999) Sediment chronology in San Francisco Bay, California, defined by ^{210}Pb , ^{234}Th , ^{137}Cs and $^{239,240}\text{Pu}$. *Mar. Chem.* **64**, 7–27.
- Gaines A. G. J. and Pilson M. E. Q. (1972) Anoxic water in the Pettaquamscutt River. *Limnol. Oceanogr.* **17**, 42–49.
- Gevao B., Hamilton-Taylor J., Murdoch C., Jones K. C., Kelly M., and Tabner B. J. (1997) Depositional time trends and remobilization of PCBs in lake sediments. *Environ. Sci. Technol.* **31**, 3274–3280.
- Goldberg E. (1962) Geochronology with ^{210}Pb . In *Symposium on Radioactive Dating*, pp. 121–131. International Atomic Energy Agency (IAEA), Greece.
- Gunten H. R. V., Sturm M., and Moser R. N. (1997) 200-year record of metals in lake sediments and natural background concentrations. *Environ. Sci. Technol.* **31**, 2193–2197.
- Hohenemser C., Deicher M., Ernst A., Hofsäss H., Lindner G., and Recknagel E. (1986) Chernobyl: An early report. *Environment* **28**, 6–13 and 30–43.
- Holloway R. W. and Liu C. K. (1988) Xenon-133 in California, Nevada and Utah from the Chernobyl accident. *Environ. Sci. Technol.* **22**, 583–586.
- Hubeny J. B. and King J. W. (2003) Anthropogenic eutrophication as recorded by varved sediments in the Pettaquamscutt River Estuary, Rhode Island, USA. In *2003 GSA Annual Meeting. Abstracts with Programs*, p. 282. GSA.
- Hughen K., Overpeck J., Anderson R. and Williams K. (1996) The potential for paleoclimate records from varved Arctic lake sediments: Baffin Island, Eastern Canadian Arctic. In *Paleoclimatology and Paleoceanography From Laminated Sediments* (ed. A. Kemp), pp. 57–71. Special Publication 116. Geological Society.
- Koide M., Bruland K., and Goldberg E. (1973) $^{228}\text{Th}/^{232}\text{Th}$ and ^{210}Pb geochronologies in marine and lake sediments. *Geochim. Cosmochim. Acta* **37**, 1171–1187.
- Krishnaswamy S., Lal D., Martin J., and Meybeck M. (1971) Geochronology of lake sediments. *Earth Planet. Sci. Lett.* **11**, 407–414.
- Lamoureux S. F. (1999) Catchment and lake controls over the formation of varves in monomictic Nicolay Lake, Cornwall Island, Nunavut. *Can. J. Earth Sci.* **36**, 1533–1546.

- Lamoureux S. (2001) Varve chronology techniques. In *Tracking Environmental Change Using Lake Sediments, Vol. 1, Basin Analysis, Coring and Chronological Techniques* (eds. W. M. Last and J. P. Smols), pp. 247–260. Kluwer.
- Larsen R. J., Sanderson C. G., Rivera W., and Zamichieli M. (1986) The characterization of radionuclides in North American and Hawaiian surface air and deposition following the Chernobyl accident. In *Environmental Measurements Laboratory: A Compendium of the Environmental Measurements Laboratory's Research Projects Related to the Chernobyl Nuclear Accident*, Vol. October 1, 1986, Report EML-460, pp. 1–104. U.S. Department of Energy.
- Levin I., Kromer B., Schoch-Fischer H., Bruns M., Münnich M., Berdau D., Vogel J., and Münnich K. (1985) 25 years of tropospheric ^{14}C observations in central Europe. *Radiocarbon* **27**, 1–19.
- Levin I. and Kromer B. (1997) Twenty years of atmospheric $^{14}\text{CO}_2$ observations at Schauinsland station, Germany. *Radiocarbon* **39**, 205–218.
- Levin I. and Heshshaimer V. (2000) Radiocarbon—A unique tracer of global carbon cycle dynamics. *Radiocarbon* **42**, 69–80.
- Lima A. L. C., Eglinton T. L., and Reddy C. M. (2003) High-resolution record of pyrogenic polycyclic aromatic hydrocarbon deposition during the 20th century. *Environ. Sci. Technol.* **37**, 53–61.
- McNichol A., Osbourne E., Gagnon A., Fry B. and Jones G. (1994) TIC, TOC, DIC, DOC, PIC, POC—Unique aspects in the preparation of oceanographic samples for ^{14}C -AMS. *Nucl. Instrum. Methods Phys. Res. B* **92**, 162–165.
- Mould R. F. (2000) *Chernobyl Record: The Definite History of the Chernobyl Catastrophe*. Institute of Physics Publishing, Philadelphia.
- NOAA. (1986) Climatological data—New England. In *Daily Precipitation*, Vol. 98. U.S. Environmental Data Service.
- Orr W. L. and Gaines A. G. J. (1973) Observations on the rate of sulfate reduction and organic matter oxidation in the bottom waters of an estuarine basin: The upper basin of the Pettaquamscutt River (Rhode Island). In *Advances in Organic Geochemistry* (eds. B. Tissot and F. Bienner), pp. 791–812. Technip.
- O'Sullivan D., Hanson Jr A., and Kester D. (1997) The distribution and redox chemistry of iron in the Pettaquamscutt Estuary. *Estuar. Coastal Shelf. Sci.* **45**, 769–788.
- Pike J. and Kemp A. E. S. (1996) Preparation and analysis techniques for studies of laminated sediments. In *Paleoclimatology and Paleooceanography from Laminated Sediments* (ed. A. E. S. Kemp), pp. 37–48. Special Publication 116. Geological Society.
- Ritchie J. and McHenry J. (1990) Application of radioactive fallout cesium-137 for measuring soil erosion and sediment accumulation rates and patterns: A review. *J. Environ. Qual.* **19**, 215–233.
- Robbins J., Holmes C., Halley R., Bothner M., Shinn E., Graney J., Keeler G., tenBrink M., Orlandini K., and Rudnick D. (2000) Time-averaged fluxes of lead and fallout radionuclides to sediments in Florida Bay. *J. Geophys. Res.* **105**, 28805–28821.
- Santschi P. H., Bollhalder S., Farrenkothen K., Lueck A., Zingg S., and Sturm M. (1988) Chernobyl radionuclides in the environment: Tracers for the tight coupling of atmospheric, terrestrial and aquatic geochemical processes. *Environ. Sci. Technol.* **22**, 510–516.
- Shapiro J. (1958) The freeze-corer—A new sampler for lake sediments. *Ecology* **39**, 74819.
- Sima O., Arnold D., and Dovlete C. (2001) GESPECOR: A versatile tool in gamma-ray spectrometry. *J. Radioanal. Nucl. Chem.* **248**, 359–364.
- Smith F. and Clark M. (1986) Radionuclide deposition from the Chernobyl cloud. *Nature* **322**, 690–691.
- Splithoff H. and Hemond H. (1996) History of toxic metal discharge to surface waters of the Aberjona watershed. *Environ. Sci. Technol.* **30**, 121–128.
- Spurr A. R. (1969) A low-viscosity epoxy resin embedding medium for electron microscopy. *J. Ultrastruct. Res.* **26**, 31–43.
- Stone R. (2001) Living in the shadow of Chornobyl. *Science* **292**, 420–426.
- Stuiver M. and Polach H. A. (1977) Reporting of ^{14}C data. *Radiocarbon* **19**, 355–363.
- Turner L. and Delorme L. (1996) Assessment of ^{210}Pb data from Canadian lakes using the CIC and CRS model. *Environ. Geol.* **28**, 78–87.
- Van Metre P., Callender E., and Fuller C. (1997) Historical trends in organochlorine compounds in river basins identified using sediment cores from reservoirs. *Environ. Sci. Technol.* **31**, 2339–2344.
- Wieland E., Santschi P., Höhener P., and Sturm M. (1993) Scavenging of Chernobyl ^{137}Cs and natural ^{210}Pb in Lake Sempach, Switzerland. *Geochim. Cosmochim. Acta* **57**, 2959–2979.
- Zwolsman J. J. G., Berger G. W., and Van Eck G. T. M. (1993) Sediment accumulation rates, historical input, postdepositional mobility and retention of major elements and trace metals in salt marsh sediments of the Scheldt Estuary, SW Netherlands. *Mar. Chem.* **44**, 73–94.